Rock Stability Analysis and Three Convergences of Discontinuous Deformation Analysis (DDA)

GEN-HUA SHI

DDA Company, 1746 Terrace Drive, Belmont, CA 94002, USA

1. Introduction

In the field of practical rock engineering, there are two independent computations: continuous computation and limit equilibrium computation. Limit equilibrium is still the fundamental method for global stability analysis. For any numerical method, reaching limit equilibrium requires large displacements, discontinuous contacts, precise friction law, multi-step computation and stabilized time-step dynamic computation. Therefore three convergences are unavoidable: convergence of equilibrium equations, convergence of open-close iterations for all contacts and convergence of the maximum displacement for static computations. This paper focuses mainly on applications of two-dimensional DDA. The applications show DDA has the ability to reach limit equilibrium of block systems. For slope or tunnel stability analyses, this paper works on rock block sliding and rotation. For dam foundation stability analysis, this paper presents dam foundation damage computation, where the block sliding is a main issue.

2. Rock Stability Computation

2.1. *About discontinuous deformation analysis (DDA)*

DDA works on block systems. Each block has linear displacements or constant stresses and strains.

The current version of 2d-DDA bas 6 unknowns per block:

x direction movement d_x,
y direction movement d_y,
rotation r_{xy},
x direction strain ε_x,
y direction strain ε_y,
shear strain τ_{xy}.

DDA uses multi-time steps. Both static and dynamic cases use dynamic computation. Static computation is the stabilized dynamic computation by applying small mount of damping. Therefore DDA can perform discontinuous and large deformation computation for both static and dynamic cases.

For each time steps, DDA usually has several open-close iterations. DDA readjust open, close or sliding modes until every contact position has the same contact mode before and after the equation solving then going to next time step. For each open-close iteration of each time step, DDA solves global equilibrium equations. The friction law is ensured in DDA computation. This law is the principle law of stability analysis. Also, the friction law is inequality equations in mathematics.

Corresponding author. E-mail: sghua@aol.com

Analysis of Discontinuous Deformation: New Developments and Applications.
Edited by Guowei MA and Yingxin ZHOU. *Published by* Research Publishing Services.

ISBN: 978-981-08-4455-4
doi:10.3850/9789810844554-keynote-Shi-Genhua

Every single block of 2-d DDA can be a generally shaped convex or concave two-dimensional polygon. Each block can have any number of edges. Based on simplex integration, the stiffness matrices, the inertia matrices, the matrices of initial stresses, the loading matrices and all other matrices of DDA are analytical solutions.

DDA has complete linear contact modes. If the time step is small enough and the total step number is large enough, DDA can simulate any possible complex movements of block systems.

DDA serves as a bridge between FEM and limit equilibrium method. DDA has strict equilibrium at each time step. After certain time step, DDA reaches dynamic or static limit equilibrium for whole simply deformable block systems.

DDA also served as implicit version of DEM method. DDA has all advantages of dynamic relaxation yet the convergence is strict and the result is accurate.

More important, DDA is a very well examined method by analytical solutions, physical model tests and large engineering projects.

2.2. *Five different factor of safety for gravity dam foundation stability analysis*

Table 1 shows the input data of three cases of dam foundation stability computation using two-dimensional DDA. Figure 1 shows the mode of failure by increasing total water pressure and reducing the friction angle. Based on the mode of failure, the sliding blocks are chosen. Based on the assumed sliding blocks, different factors of safety are computed. In Table 1, three cases are included:

Case 1 is limit equilibrium method. Here normal loads are applied, the factor of safety of the chosen sliding blocks are computed. The factor of safety is 1.94 as shown in Table 1.

Case 2 is the fictitious force method. Keeping the stability, increase the water pressure as much as possible. The factor of safety is the ratio of applied total water pressure and the total normal water pressure. The factor of safety is 2.80 as shown in Table 1.

Case 3 is the strength reduction method. Keeping the stability, reducing the friction angle as much as possible. The factor of safety is the ratio of the tangent of real friction angle and the tangent of reduced friction angle. The factor of safety is 2.91 as shown in Table 1.

Table 1. Physical data of rock mass of gravity dam foundation.

Material parameters	1. Limit equilibrium	2. Fictitious force	3. Strength reduction
Unit weight	2.4	2.4	2.4
Elastic Modulus	2600000	2600000	2600000
Poisson's ratio	0.25	0.25	0.25
Friction angle	17.0	17.0	6.0
Cohesion	0.0	0.0	0.0
Additional water pressure	0.0	7290	0.0
Dynamic ratio	0.9999	0.999	0.999
Contact stiffness	10000000	5000000	10000000
Time interval	0.05	0.05	0.05
Total time step	1500	1500	1500
Ending max. displ. ratio	<0.0000005	<0.0000005	<0.0000005
Factor of safety	1.94	2.80	2.91
Margin factor of safety	+0.0	+0.14	+0.39

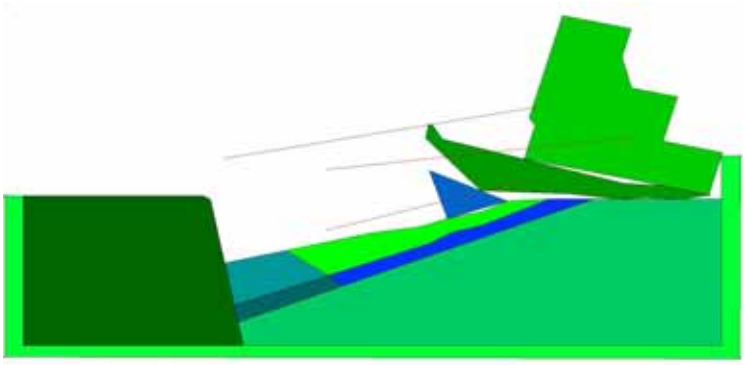

Figure 1. Dam foundation failure with increased water pressure and reduced friction angle.

Case 4 is the limit equilibrium method under the fictitious force. All parameters are the same as case 2. The computation is also identical with case 2. After increasing the water load, the computed factor of safety FS is still greater than 1.0. The resulting factor of safety is the factor of safety of case 2 plus the marginal factor of safety $FS - 1.0 = 0.14$.

Case 5 is the limit equilibrium method under the reduced friction angle. All parameters are the same as case 3. The computation is also identical with case 3. After reducing the friction angle, the computed factor of safety FS is still greater than 1.0. The resulting factor of safety is the factor of safety of case 3 plus the marginal factor of safety $FS - 1.0 = 0.39$.

The dynamic ratio is 0.9999 in case 1 for example. It means the next time step inherent 99.99% of the velocity from the previous time step.

The maximum displacement ratio is the allowed maximum step displacement divided by the half height of the whole mesh. In Table 1, the maximum displacement ratio is less than 0.0000005.

The unified units on weight, length, time and angle are the following:

Weight unit: Ton
Length unit: meter
Time unit: second
Angle unit: degree

The computation results of all case 1 to case 5 are stable. All case 1 to case 5 didn't reach limit equilibrium. Except case 1, all case 2 to case 5 are close to limit equilibrium. Figure 2 shows the results of all case 1 to case 5. The computation requirement of case 2 to case 5 is highly difficult because these cases are very close to limit equilibrium or very close to failure. The computation of case 2 to case 5 also requires three convergences.

2.3. *Rock falling of underground power chambers*

In the following, sections of a given underground powerhouse are analyzed by two-dimensional DDA. The underground powerhouse section has two cases: without bolt support and with bolt support. All two cases are based on the same geometric data of joint sets shown by Table 2. Table 3 shows the physical data of the underground chamber rock mass.

The rock falling computation of underground chamber (Figures 3–4) uses two-dimensional DDA. Total 1800 time steps are used. In the cases of Figure 2 and 3, the time interval was

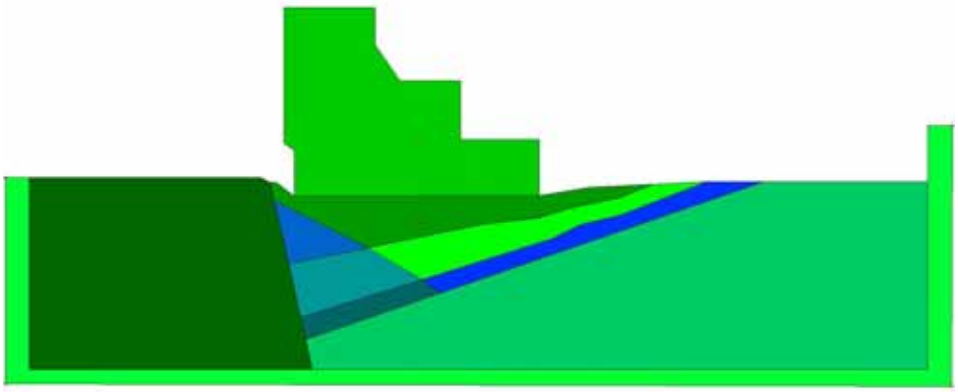

Figure 2. Result of dam foundation of case 1 to case 5.

automatic chosen and controlled by maximum displacement ratio 0.001. In the cases of Figures 3 and 4, the dynamic ratio is 1.0. It means in the beginning of the next time step 100% of velocity is inherited from the present time step. Therefore rock falling computation is fully dynamic without damping.

The geometric data of joint sets of the underground power chamber for Figure 3–6 are shown in Table 2.

The physical data of the rock mass of Figures 3–4 are shown on Table 3.

Figures 3 and 4 show rock fall process and final state of this underground powerhouse.

Table 2. Geometric data of joint sets of the underground power chamber.

Joint set	1	2	3
Dip angle	35 degree	70 degree	85 degree
Dip direction	315 degree	150 degree	25 degree
Average spacing	6.0 meter	4.0 meter	3.0 meter
Average length	100 meter	20 meter	30 meter
Average bridge	0.2 meter	1.0 meter	0.5 meter
Degree of random 0.0–1.0	0.5	0.5	0.5

Table 3. Physical data of underground chamber rock mass.

Material parameters	Parameters	Computation data	Data
Unit weight	2.7	Dynamic ratio	1.0
Elastic Modulus	3000000	Contact stiffness	1000000
Poisson's ratio	0.25	Time interval	Automatic
Friction angle	25	Total time step	1800
Cohesion	0	Ending max. displ. ratio	0.48

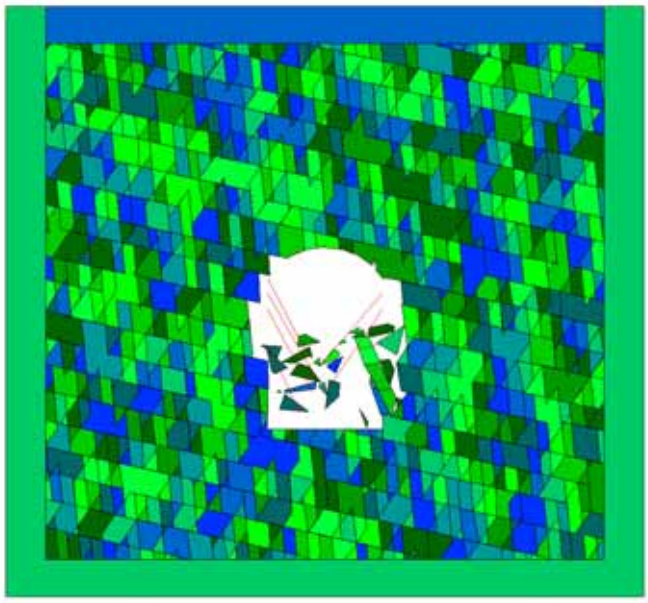

Figure 3. Rock falling process of the underground powerhouse computed by 2-d DDA without bolt support.

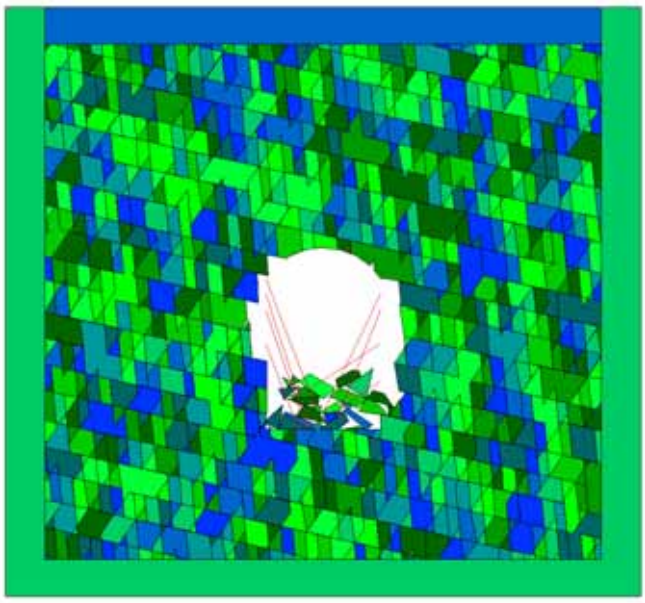

Figure 4. Rock falling final condition of the underground powerhouse computed by 2-d DDA without bolt support.

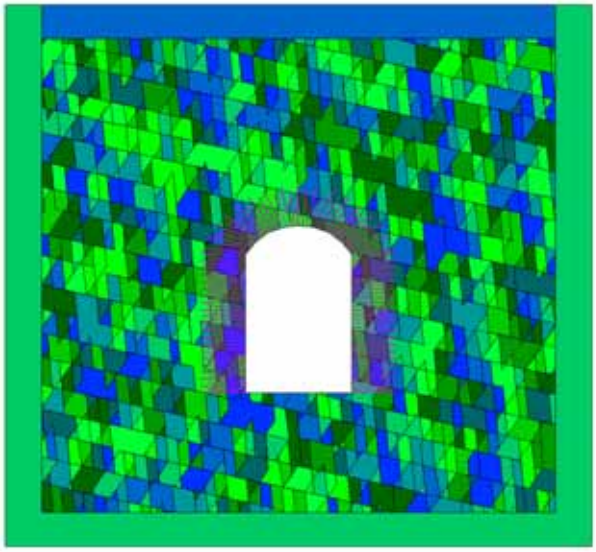

Figure 5. Bolting computation of underground powerhouse where the location of each bolt is drawn.

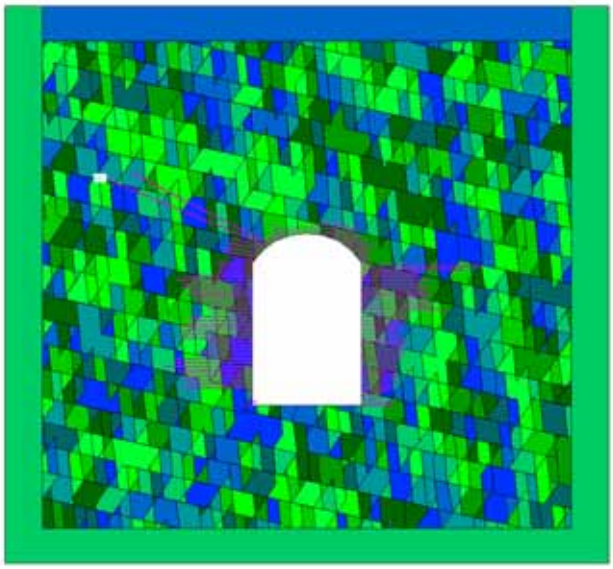

Figure 6. Bolting forces of the underground powerhouse where the force of each bolt is drawn as the length along this bolt.

2.4. *Rock bolting of an underground power chamber*

The rock bolting computation of the underground chamber (Figures 5–6) uses two-dimensional DDA. Total 2000 time steps are used. The time interval was not controlled by maximum displacement ratio. The step time interval is 0.002 seconds. The dynamic ratio is 0.97.

Table 4. Physical data of underground chamber rock mass.

Material parameters	Parameter	Computation data	Data
Unit weight	2.7	Dynamic ratio	0.97
Elastic modulus	3000000	Contact stiffness	3000000
Poisson's ratio	0.25	Time interval	0.002
Friction angle	25	Total time step	2000
Cohesion	0	Ending max. displ. ratio	0.000026
Bolt stiffness	16889	Max. bolting force error	<0.0000005

It means in the beginning of the next time step 97% of velocity is inherited from the present time step. This miner volume damping can obtain stabilized contact forces. The forces of all bolts are highly stabilized. The bolting forces were not changed in 6 digits after the dismal point under large enough time steps.

The physical data of the rock mass of Figures 5–6 are shown on Table 4.

Figure 5 shows the location of each rock bolts. The length of the rock bolts are 10 meter and 12 meters alternatively. The bolt spacing is one meter. The diameter of the rock bolts is 32 mm.

Figure 6 shows the bolting forces of the underground powerhouse where the force of each bolt is drawn as the length along this bolt.

Figure 7 is the time depending resulting bolting forces (unit ton) of bolt number 1 to 30 counting from top centre down and right to left in each level of the underground power house section. From bolt 1 to bolt 30, there are two bolts where the tension forces exceed 25 tons as shown by Figure 7.

Figure 8 is time depending resulting bolting forces (unit ton) of bolt number 31 to 60 counting from top centre down and right to left in each level of the underground power house section. It can be seen that, there are two bolts where the tension forces are greater than 25 tons.

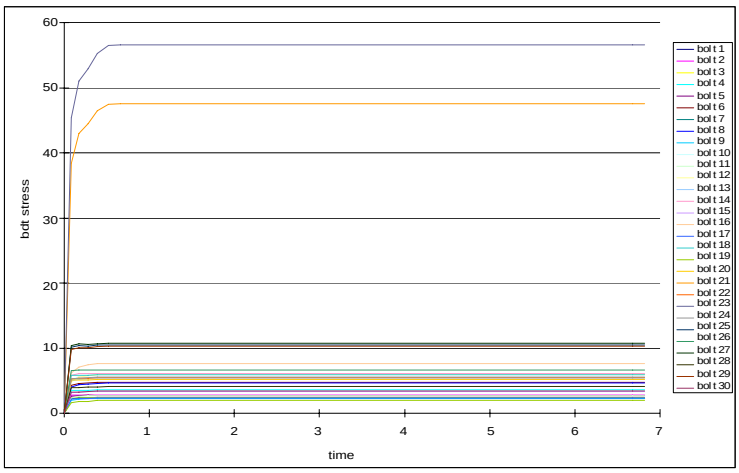

Figure 7. Time depending resulting bolting forces of bolt number 1 to 30 counting from top centre down and right to left in each level of the underground power house section.

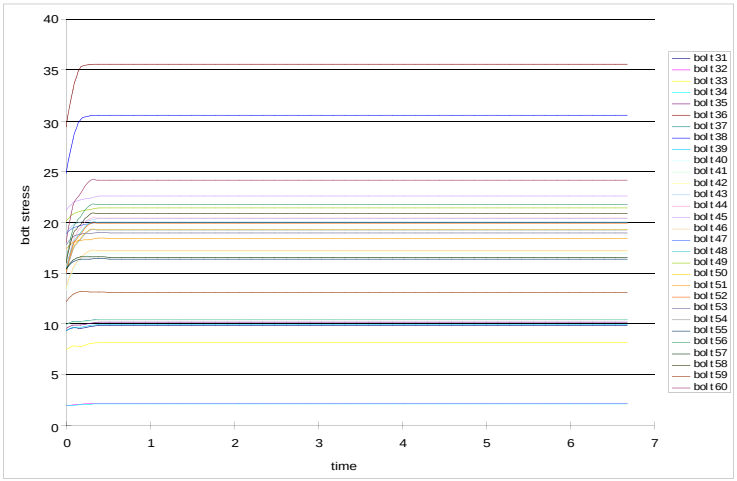

Figure 8. Time depending resulting bolting forces of bolt number 31 to 60 counting from top centre down and right to left in each level of the underground power house section.

Figure 9 is time depending resulting bolting forces (unit ton) of bolt number 61 to 90 counting from top centre down and right to left in each level of the underground power house section. It can be seen from Figure 9 that, there is no blot where the tension force is greater than 25 tons.

Figure 10 is the time depending resulting bolting forces (unit ton) of bolt number 91 to 115 counting from top centre down and right to left in each level of the underground power house section. It can be seen that, there is only one bolt where the tension force is greater than 25 tons.

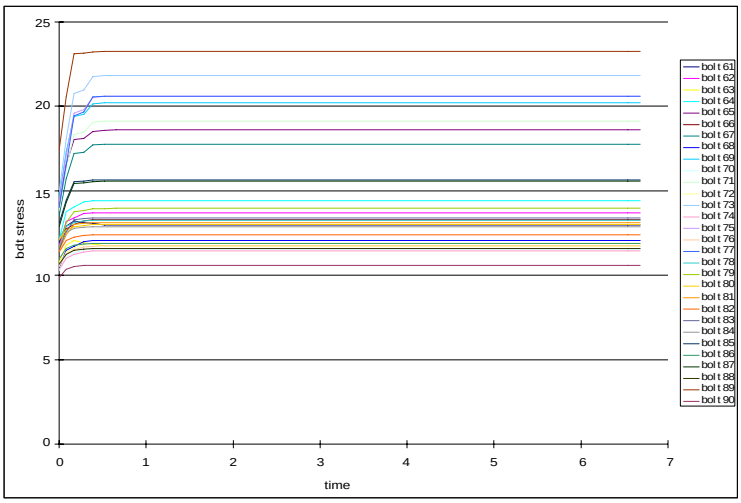

Figure 9. Time depending resulting bolting forces of bolt number 61 to 90 counting from top centre down and right to left in each level of the underground power house section.

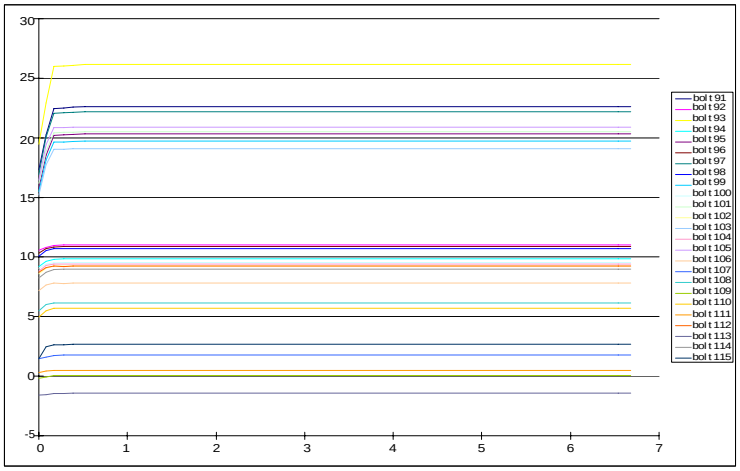

Figure 10. Time depending resulting bolting forces of bolt number 91 to 115 counting from top centre down and right to left in each level of the underground power house section.

Table 5. Geometry and physical data of joint set.

Joint set	Dip angle	Average spacing	Average length	Cohesion	Friction angle
1 (foliation)	70 degree	7 ft	2000 ft	0 psf	10 degree
2	20 degree	30 ft	30 ft	0 psf	30 degree

Weight unit: Ton
Length unit: meter
Time unit: second
Angle unit: degree

2.5. *Stability computation of toppling slopes: foliation planes have 70 degrees dip angle*

From the drilling data, the original dip angle of the foliation planes is about 70 degrees. If after toppling, the second joint set has 40 degrees dip angle, the original dip angle of the second joint set is about 20 degrees. The following Table 5 includes the geometric data and physical data of the joint sets and rock masses. The following computation is to simulate or back calculate the past toppling of the slope.

Figure 11 shows the result of the slope, the dip angle of the foliation planes is 70 degrees.

Figure 12 is the time depending movements of the measured points under the anchor block of the slope for the previous case of Figure 11.

Computation of two-dimensional DDA uses 30000 time steps, 0.002 second per step. The dynamic ratio is 0.99. It means the next time step inherent 0.99 of the velocity from the previous time step. Under the 70 degrees dip angle of the foliation planes, the toppling of the slope is very large. It can be seen; the slope is convex which gives more room for block rotation or toppling.

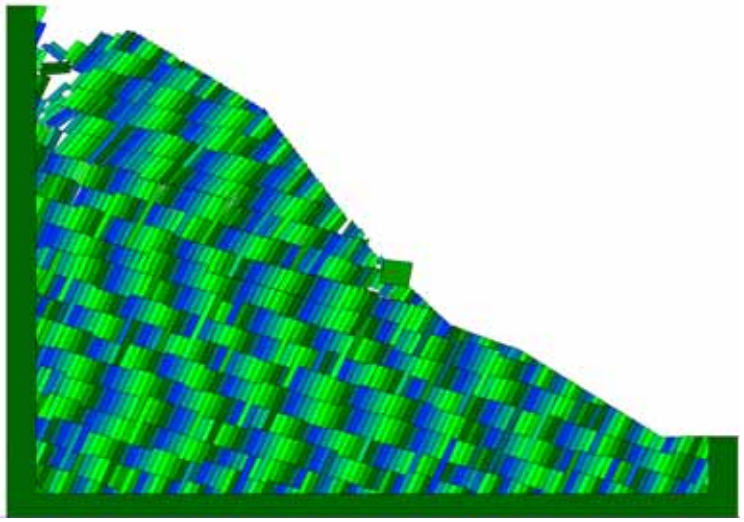

Figure 11. Toppling of the slope where the dip angle of foliation plane is 70 degrees.

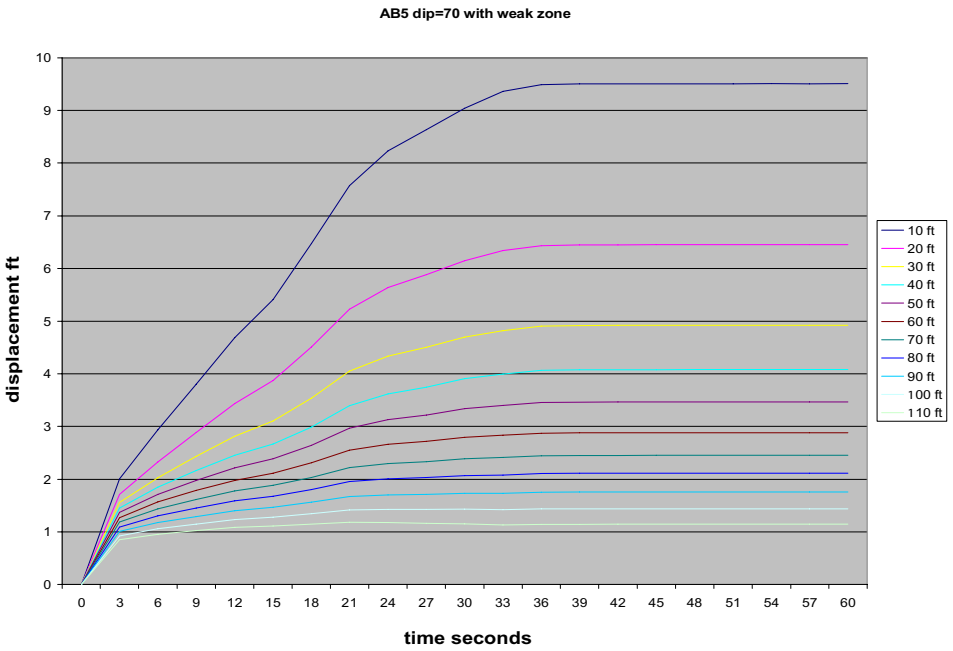

Figure 12. Displacements of points under the slope where the dip angle of foliation planes is 70 degrees.

Figure 11 shows that, after large mount of rotation, the toppling reached a stable state. Therefore the toppling mode is different from the sliding mode. Generally speaking, the toppling mode can be stabilized after the rotation. For sliding mode, as soon as the slope start to slide, the sliding can hardly to stop.

Acknowledgements

The project of "Discontinuous Deformation Analysis (DDA) of Block Systems" (XDS2007-10) provided financial support to this research.

References

1. Shi, Gen-hua, *Block System Modelling by Discontinuous Deformation Analysis*, *Computational Mechanics Publications*, New Southampton, UK and Boston, USA, 1993.
2. Shi, Gen-hua, "Single and Multiple Block Limit Equilibrium of Key Block Method and Discontinuous Deformation Analysis", *Stability of Rock Structures*, *ICADD-5*, Beer Sheva, Israel. 3–46, 2002.
3. Shi, Gen-hua, "Applications of Discontinuous Deformation Analysis (DDA) and Manifold Method", *The Third International Conference on Analysis of Discontinuous Deformation, ICADD-3*, Vail, Colorado, USA, 1999, 3–15.